PCCP

PAPER

View Article Online
View Journal | View Issue

Cite this: *Phys. Chem. Chem. Phys.*, 2017, **19**, 32473

Termination of Ge surfaces with ultrathin GeS and GeS_2 layers *via* solid-state sulfurization†

Hui Chen, [ab] Courtney Keiser, [c] Shixuan Du, [b] Hong-Jun Gao, [b] Peter Sutter *[a] and Eli Sutter *[c]

Received 2nd September 2017,
Accepted 24th November 2017

DOI: 10.1039/c7cp05990f

rsc.li/pccp

Reactions of Ge with S vapor, of interest as a potential approach for forming thin passivation layers on Ge surfaces, have been studied by photoelectron spectroscopy and Raman spectroscopy. Exposure of Ge(100) and Ge(111) to S drives the formation of Ge sulfide near-surface layers. At low temperatures, the reaction products comprise a thin GeS interlayer terminated by near-surface GeS_2. Above 400 °C, exposure to sulfur gives rise to single-phase GeS_2 layers whose thickness increases with temperature. Arrhenius analysis of the GeS_2 thickness yields an activation energy (0.63 ± 0.08) eV, close to the barrier that controls Ge oxidation by O radicals. XPS measurements after extended ambient exposure show a stable, ultrathin near-surface GeS_2 without significant oxidation, indicating that Ge–sulfides may provide an effective surface passivation for Ge surfaces.

Introduction

Silicon owes much of its widespread use in the semiconductor industry to the stability of its native oxide and the excellent passivation achieved for oxide-covered surfaces.[1,2] Alternative materials to Si often lack a stable, well-passivating oxide and their viability as electronic materials depends on the development of suitable terminations that offer protection from reactive species in air and provide a low density of electronic defect states at the surface.[3] Surface passivation by chalcogens (*i.e.*, sulfur or selenium) is attractive since it can potentially endow the surface of 3D semiconductors with properties that are similar to those of 2D metal chalcogenides, notably a very low chemical reactivity and complete elimination of dangling bonds. A prominent example of a semiconductor for which passivation by sulfur has shown promising results is germanium. Ge is attractive due to its substantially higher charge carrier mobility than in Si[4] and a good lattice match with GaAs that can facilitate materials integration for high-performance electronics and optoelectronics, but its oxides are unstable and have poor electronic properties. Passivation of Ge(100) by chemisorption of elemental S to 1 monolayer (ML) coverage in ultrahigh vacuum was shown to produce a Ge(100)-(1 × 1)-S surface that is remarkably resistant to oxidation in air.[3,5,6] Repeated dissociative adsorption of H_2S causes S atoms to occupy the same (bridge) sites on Ge(100)-(2 × 1) but the S coverage saturates at 0.5 ML instead of 1 ML for direct adsorption of S.[7] Alternative approaches for realizing a sulfur-terminated surface involve the deposition of S from aqueous solution. Treatment of Ge(100) surfaces as well as Ge nanowires by aqueous $(NH_4)_2S$ yielded different reported results, ranging from (1 × 1)-S surface adsorption[8] to the formation of thicker glassy GeS_x layers,[9,10] but the resulting surface passivation proved invariably effective in resisting oxidation in air.[8–11]

Inspired by the effective passivation of Ge surfaces by thin layers of amorphous GeS_x formed by aqueous treatments, we investigated a different approach to producing Ge–sulfides on Ge(100): solid-state reactions involving exposure to S vapor at elevated substrate temperatures and near atmospheric pressure. Recently, the direct sulfurization of transition metals surfaces has been reported as a way of producing high-quality few-layer and monolayer MoS_2[12–15] and WS_2.[16] We report a study on the formation of GeS and GeS_2 ultrathin films by direct sulfurization of Ge(100). We analyze the reaction kinetics and derive the activation energy of the rate-limiting step of the sulfurization reaction through X-ray photoelectron spectroscopy (XPS) and Raman spectroscopy on samples exposed to the same S dose at different temperatures. Our results show that the sulfurization process gives rise to two GeS_x phases. Low-temperature reactions yield ultrathin films of mixed GeS and GeS_2, whereas at higher temperatures a transition to thicker films consisting of pure GeS_2 is observed. The thickness evolution of the high-temperature stable GeS_2 layer follows an Arrhenius behavior with activation energy of E_A = 0.68 eV, which

[a] *Department of Electrical & Computer Engineering, University of Nebraska-Lincoln, Lincoln, NE 68588, USA. E-mail: psutter@unl.edu*
[b] *Institute of Physics & University of Chinese Academy of Sciences, Chinese Academy of Sciences, Beijing 100190, P. R. China*
[c] *Department of Mechanical & Materials Engineering, University of Nebraska-Lincoln, Lincoln, NE 68588, USA. E-mail: esutter@unl.edu*

† Electronic supplementary information (ESI) available. See DOI: 10.1039/c7cp05990f

we attribute to a reaction-limiting diffusion process through the sulfide layer. Our results demonstrate the ability of controllably producing Ge–sulfide passivation layers on Ge(100) *via* solid-state reactions in S vapor near ambient-pressure.

Methods

Ge surfaces were reacted with sulfur in a two-zone tube furnace with a 2-inch quartz tube and an additional internal liner consisting of a section of smaller diameter quartz tubing. Sulfur powder (99.9995%, Alfa Aesar) held in a quartz boat was placed in the upstream zone. Ge(100) substrates rinsed in deionized (DI) water to remove the native germanium oxide were placed in the downstream zone. The furnace was pumped by a mechanical pump, and a $Ar:H_2$ gas mixture (ratio: 95 : 5) was used as carrier gas with a flow rate of 50 sccm. The sulfur reservoir was heated to a temperature of 150 °C to establish a vapor pressure of ~0.3 Torr.[17] The data shown in Fig. 4 were obtained on samples exposed to lower sulfur pressure (120 °C reservoir, ~0.03 Torr) to probe the early reaction stages. The sample temperature was varied between 260 °C and 460 °C to probe reaction kinetics and products as a function of temperature. Solid-state reactions were performed at constant temperature of sample and source, obtained by ramping the furnace so that the target temperatures were reached simultaneously and held for a defined time (10 minutes), immediately followed by cooling to room temperature at natural rate.

Following the reaction with sulfur, the samples were transferred through air into an ultrahigh vacuum (UHV) chamber for X-ray photoelectron spectroscopy (XPS). XPS was measured with a non-monochromated laboratory X-ray source (SPECS XR50; Al Kα line, $h\nu$ = 1486.7 eV) at a power of 180 W (12 kV, 15 mA). Photoelectrons were detected in a hemispherical energy analyzer equipped with multi-channeltron detector (SPECS Phoibos 100 MCD-9). Wide-scan survey spectra and high-resolution spectra of Ge 3d, Ge 2p, S 2p and C 1s core-levels were collected. For each sample, binding energies were calibrated to a C 1s reference from adventitious carbon, set to 285.0 eV.[18] Casa XPS analysis software was used to perform peak fitting (Gaussian (70%)–Lorentzian (30%) product with Shirley background) to deconvolute the different components contributing to the measured spectra, and to determine the stoichiometry of samples from fitted peak areas. Ge 3d and Ge 2p spectra were fitted to a minimum number of components that provided good fits and could be justified by comparison with reference spectra and published peak assignments. Generally, no restrictions were placed on peak position, area, or width and different initial conditions were used to test convergence to a stable global minimum. For the S 2p peaks, a fixed branching ratio of 0.5 was imposed between the S $2p_{1/2}$ and S $2p_{3/2}$ peak areas. Reference samples of oxide-free Ge(100), GeS, and GeS_2 powders were measured using the same conditions to support the assignment of XPS peaks and the thickness determination of the near-surface phases formed by reaction with sulfur. Micro-Raman spectroscopy of the Ge(100) reacted with S was carried out using a Raman microscope (Renishaw InVia) with an excitation wavelength of 532 nm and a lateral resolution of ~1 μm. Each reported Raman spectrum corresponds to the accumulation of tens of individual spectra recorded at different random sample locations to avoid possible effects due to damage by laser exposure and to obtain a better signal-to-noise ratio. Scanning electron microscopy (SEM) was performed in a FEI Helios Nanolab 660 with a field emission gun at 2 kV.

Results and discussion

The state of the starting surface is important for solid-state reactions, such as the Ge sulfurization reaction considered here. A characterization of the Ge substrate preparation by XPS is shown in the ESI† (Fig. S1). It compares surface sensitive Ge 2p XPS spectra (kinetic energy ~ 267 eV) of a Ge(100) substrate in the as-received state (*i.e.*, with native oxide) and after rinsing with DI water. The initial spectrum shows an intense peak with binding energy BE = 1220.6 eV, consistent with Ge^{4+} in GeO_2 along with a small Ge^0 component (BE = 1217.6 eV). After rinsing with DI water, the Ge^{4+} peak is no longer detectable, and the dominant signal is now due to Ge^0 (BE = 1217.6 eV). A small peak at 1219.6 eV is assigned to sub-oxides (other than GeO_2). These findings are consistent with published results on the preparation of Ge surfaces by DI water rinsing,[19–21] which showed that GeO_2 is water soluble and therefore completely removed by H_2O rinsing whereas GeO and GeO_x ($x < 2$) sub-oxides are insoluble and remain as traces on the surface. In the present case, the estimated residual GeO_x surface coverage is below 15% based on the measured peak areas in Fig. S1 (ESI†). Exposure to sulfur at high temperatures should further reduce these remaining trace oxides at the onset of the solid-state reactions.

Fig. 1 shows results of an XPS analysis of the sulfurization of Ge(100) at different reaction temperatures. Ge 3d XPS spectra obtained on Ge(100) samples exposed to sulfur at different temperatures (Fig. 1(a)) can be fitted by a series of three distinct peaks. The dominant component at low reaction temperatures with binding energy of 30.4 eV is attributed to Ge^0 signal from the Ge substrate, based on XPS measurements on an oxide-free Ge reference sample (Fig. 1(b)) and comparison with published results.[22–24] The assignment is further corroborated by the progressive attenuation of this peak by the thickening sulfur-rich surface layer at higher reaction temperatures. Based on XPS spectra of GeS and GeS_2 reference samples shown in Fig. 1(b), the component at the highest binding energy (32.2 eV) is associated with Ge in a (+4) oxidation state, *i.e.*, GeS_2. The component at intermediate binding energy results from Ge with an oxidation state of (+2), *i.e.*, GeS. As the reaction temperature is increased, the intensity of the GeS_2 peak increases whereas the GeS component decreases and vanishes at ~420 °C (Fig. 1(a)). S 2p spectra can be fitted by two peaks, which we assign to S $2p_{1/2}$ and $2p_{3/2}$, respectively (Fig. 1(c)). At higher reaction temperatures, the S $2p_{3/2}$ peak becomes narrower and shifts from 162.45 eV to 163.10 eV, indicating that the chemical state of sulfur becomes

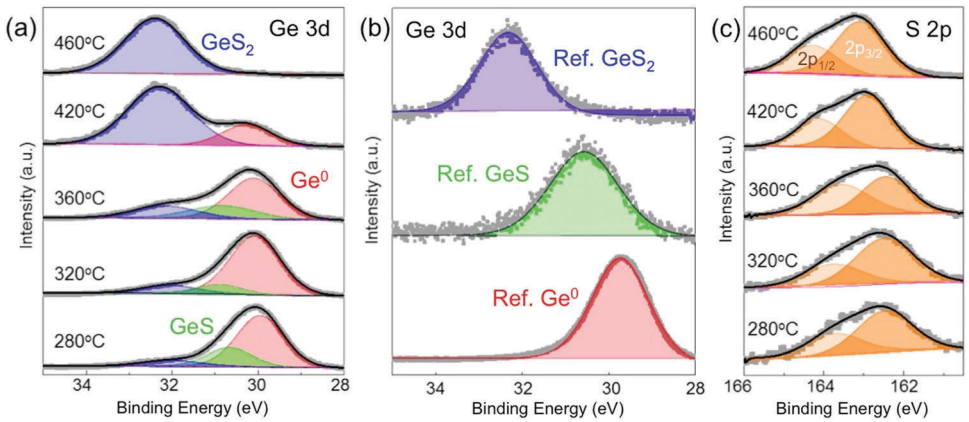

Fig. 1 XPS of germanium sulfide films produced *via* reaction of Ge(100) with sulfur vapor at temperatures between 280 °C and 460 °C. (a) Evolution of Ge 3d core-level spectra, fitted by three peaks: elemental germanium (Ge^0, red), binding energy BE = (30.2 ± 0.2) eV, and two peaks assigned to higher oxidation states of Ge:Ge^{2+} (GeS, green), BE = (30.9 ± 0.2) eV, and Ge^{4+} (GeS_2, blue), BE = (32.2 ± 0.2) eV. Gray symbols: measured data. Black line: global fit. (b) Ge 3d reference spectra from a Ge(100) wafer rinsed in DI water, and from GeS and GeS_2 powders. (c) Evolution of S 2p core-level spectra with fits to S $2p_{1/2}$ (light yellow), BE = (164.0 ± 0.3) eV, and S $2p_{3/2}$ (dark yellow), BE = (162.8 ± 0.3) eV.

more uniform at higher temperatures consistent with the development of a single predominant (GeS_2) near-surface phase.

The thickness of the GeS and GeS_2 components of the sulfurized surface layer was determined within the framework of a three-layer model (Fig. 2(a) inset), which assumes that an outermost layer with high sulfur content (*i.e.*, GeS_2) is separated from the unreacted Ge substrate by an intermediate phase with lower sulfur concentration (*i.e.*, GeS). This scenario is similar to other solid-state reactions in materials systems for which stable phases with different stoichiometry exist, *e.g.*, reactions of silicon with transition metals such as nickel or cobalt to form silicides.[25] In the case of $NiSi_x$, for example, it has been shown that Si rich and Ni rich phases coexist and are separated by a well-delineated front.[26,27]

To quantify the different layer thicknesses, we analyzed the Ge 3d XPS intensity originating from Ge in GeS, GeS_2 and the Ge substrate. Each layer is characterized by a sensitivity factor

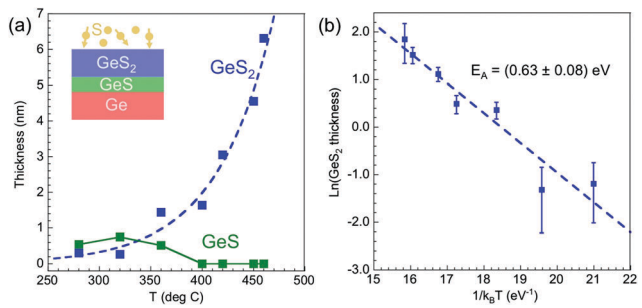

Fig. 2 Analysis of the XPS data and activation energy of the sulfurization of Ge(100). (a) Evolution of GeS and GeS_2 thickness (t) with reaction temperature, based on a quantification of the XPS data of Fig. 1 within a three-layer model (inset) as described in the text. The solid line is a guide to the eye; the dashed line is an exponential fit to the data for $t(GeS_2)$. (b) Arrhenius plot of the thickening of the GeS_2 film. The data can be fitted by a thermally activated behavior with activation energy E_A = (0.63 ± 0.08) eV. Error bars are based on an error analysis as described in the ESI.†

$S = \sigma L n \lambda \cos(\theta) Q(E)$, where σ is the photoelectron cross-section, L the angular asymmetry of photoemission intensity for each atom, n the atomic density of Ge in the layer, θ the emission angle with respect to the surface normal, and $Q(E)$ the (kinetic energy dependent) intensity response function of the spectrometer. For Al-Kα excitation, the inelastic mean free path of Ge3d photoelectrons (kinetic energy ~ 1450 eV) is $\lambda \sim 1.1$ nm.[28,29] Generally, the intensity of photoelectrons $I(t)$ emitted from a surface covered by a layer of thickness t is given by the Beer–Lambert equation:

$$I(t) = J \cdot S \exp\left[-\frac{t}{\lambda}\right] \quad (1)$$

where J is the intensity of the incident X-ray radiation (the product $J{\cdot}S$ denotes the photoelectron intensity $I(t = 0)$ without the attenuating layer). For the three-layer system considered here, photoelectrons from the Ge substrate are attenuated by both the GeS and GeS_2 layers:

$$I_{Ge} = JS_{Ge} \exp\left[-\frac{t(GeS)}{\lambda}\right] \cdot \exp\left[-\frac{t(GeS_2)}{\lambda}\right] \quad (2)$$

The XPS intensity from the intermediate GeS layer increases with GeS thickness, and it is attenuated by the GeS_2:

$$I_{GeS} = JS_{GeS}\left(1 - \exp\left[-\frac{t(GeS)}{\lambda}\right]\right) \cdot \exp\left[-\frac{t(GeS_2)}{\lambda}\right] \quad (3)$$

Finally, the intensity of the outermost GeS_2 layer depends only on its own thickness: $I_{GeS_2} = JS_{GeS_2}\left(1 - \exp\left[-\frac{t(GeS_2)}{\lambda}\right]\right)$. These equations can be solved for the thickness of the GeS and GeS_2 layers:

$$t_{GeS} = \lambda \cdot \ln\left(1 + \frac{I_{GeS}/S_{GeS}}{I_{Ge}/S_{Ge}}\right) \quad (4)$$

$$t_{GeS_2} = \lambda \cdot \ln\left(1 + \frac{I_{GeS_2}/S_{GeS_2}}{I_{Ge}/S_{Ge}} \cdot \exp\left(-\frac{t(GeS)}{\lambda}\right)\right) \quad (5)$$

The sensitivity factors S_{GeS_2}, S_{GeS} and S_{Ge} are equal except for different atomic densities of Ge in the two Ge sulfide phases and the crystalline Ge substrate. To quantify the thickness t_{GeS_2} and t_{GeS} values of Ge atomic densities n_{Ge} = 41.8 at nm^{-3}, n_{GeS} = 23.6 at per nm^3, and n_{GeS_2} = 11.3 at per nm^3 were used, derived from calculated mass densities of Ge, GeS, and GeS_2 reported in Materials Project.[30] We note that one might consider the possible existence of a thin S film on the surface as a fourth layer. Neither the experimental protocol nor the XPS results support the existence of such a film, but any additional (non-Ge containing) surface layer would merely cause a global attenuation of all Ge 3d intensities without affecting the conclusions from our analysis of Ge 3d XPS spectra. Future work will address possible other effects, *e.g.*, any developing surface or interface roughness, which are neglected in our present analysis. For the small thicknesses of the reacted layers considered here (<10 nm), we expect such effects to be negligible.

Fig. 2(a) shows the thickness of the Ge–sulfide layers on Ge(100) formed at different reaction temperatures. The interfacial GeS layer is generally very thin (below 1 nm). Its thickness decreases above 320 °C and it can no longer be detected for reaction temperatures of 400 °C and above. The absence of this phase at elevated temperatures is consistent with the low thermal stability of GeS, reported previously.[31] In contrast the thickness of GeS_2, which is stable to much higher temperatures,[31] increases monotonically with temperature and reaches values greater than 6 nm at 460 °C for our standard reaction conditions (10 min S exposure at 0.3 Torr vapor pressure). The analysis shown in Fig. 2(a) based on the analysis of Ge 3d XPS spectra is further corroborated by surface sensitive Ge $2p_{3/2}$ spectra obtained on the same samples (Fig. S2, ESI†). The Ge $2p_{3/2}$ spectra show a very small residual Ge^0 component at the lowest reaction temperature (280 °C), an intermediate regime in which GeS and GeS_2 coexist, and ultimately the complete replacement of GeS by GeS_2 at the highest temperatures.

The measured t_{GeS_2} can be fitted well by an exponential dependence on the reaction temperature (Fig. 2(a)). Fig. 2(b) shows an Arrhenius analysis, in which the rate constant of the reaction-limiting step is represented by the GeS_2 thickness. The analysis suggests a dependence $t_{GeS_2} \sim \exp\left(\frac{-E_A}{k_B T}\right)$ with activation energy E_A = (0.63 ± 0.08) eV (k_B denotes Boltzmann's constant and T is the absolute temperature). Similar to other solid-state reactions, such as oxidation or nitridation, the thickening of the GeS_2 layer due to reaction with sulfur requires mass transport of at least one species (here Ge or S) through the surface layer. In such a scenario, bulk diffusion is a likely thermally activated (reaction limiting) step at a later stage of the solid-state reaction (*i.e.*, when a Ge–sulfide layer presents a diffusion barrier against further reaction with sulfur), and the presence of a less sulfur-rich GeS interlayer, at least at low reaction temperatures, suggests that the primary diffusing species is S. It is instructive to compare the activation energy with that controlling Ge oxidation. In the parabolic growth regime within the Deal–Grove model,[32] *i.e.*, the stage in which oxide growth is limited by diffusion of oxygen through GeO_x,

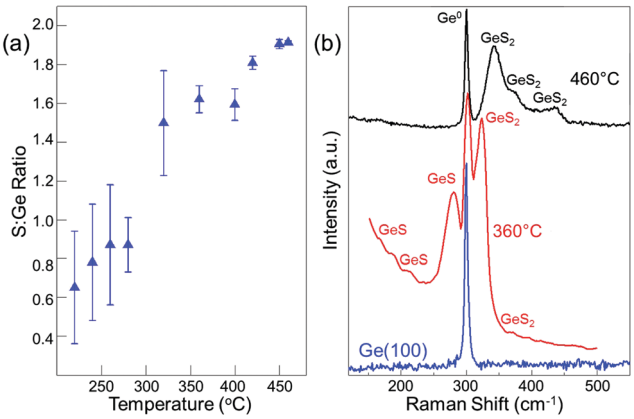

Fig. 3 Overall Ge : S ratio and Raman spectra of the GeS/GeS_2 layers resulting at different growth temperatures. (a) Stoichiometric ratio of Ge and S evaluated from of Ge 3d and S 2p XPS spectra. (b) Raman spectra of germanium sulfide films formed at reaction temperatures of 360 °C and 460 °C, along with a reference spectrum of the Ge(100) substrate.

thermal oxidation in O_2 at low pressures involves a significantly higher activation energy ($E_A \sim 1.7$ eV)[33] than found here for the formation of near-surface GeS_2. However Ge oxidation in ozone, which is thought to involve O radicals that are readily generated by the facile dissociation of O_3 on the surface, is in the same (parabolic) regime governed by a significantly reduced activation energy, E_A = 0.54 eV,[34] which is close to the E_A found here for reaction with S vapor at comparable temperatures.

Based on the integrated intensities of the relevant Ge 3d and S $2p_{3/2}$ components and taking into account the relative sensitivity factors of the different core levels (Ge 3d: 0.433; S $2p_{3/2}$: 0.300),[35] we evaluated the ratio of [S] : [Ge] following reaction with sulfur at different temperatures (Fig. 3(a)). At temperatures between 220 °C and 280 °C, the stoichiometric ratio of S and Ge is close to 1. As the reaction temperature increases, the ratio rises from ~1 at 300 °C to values near 2 at 460 °C, in good agreement with the conclusions reached in our thickness analysis within a two-layer model.

To further study the evolution of the GeS_x phases with temperature, we measured Raman spectra on samples reacted at different temperatures. Fig. 3(b) shows typical Raman spectra of Ge(100) samples exposed to sulfur at temperatures of 360 °C and 460 °C, respectively. The higher temperature (460 °C) sample shows three peaks at 342 cm^{-1}, 374 cm^{-1} and 437 cm^{-1}. These three peaks are consistent with the A_1 symmetric breathing mode of corner-sharing [$(GeS_{1/2})_4$] tetrahedral units, A_c^1 companion vibrations in edge sharing [$(GeS_{1/2})_4$] tetrahedral units, and an S–S stretch mode from cluster edge dimers in GeS_2, respectively.[36] The spectrum thus indicates that the near-surface layer in this sample primarily consists of GeS_2 phase. For the sample grown at 360 °C, there are again three peaks above 300 cm^{-1} corresponding to the Raman modes of GeS_2, but two of these three peaks are much weaker and all three are shifted to lower wavenumbers. In addition, three peaks appear below 300 cm^{-1}, and are located at 190 cm^{-1}, 216 cm^{-1} and 278 cm^{-1}, respectively. We attribute these peaks to the in-plane shearing mode B_{3g} (190 cm^{-1}), out-of-plane compressive mode B_{2g} (216 cm^{-1}) and in-plane shearing mode A_{1g}

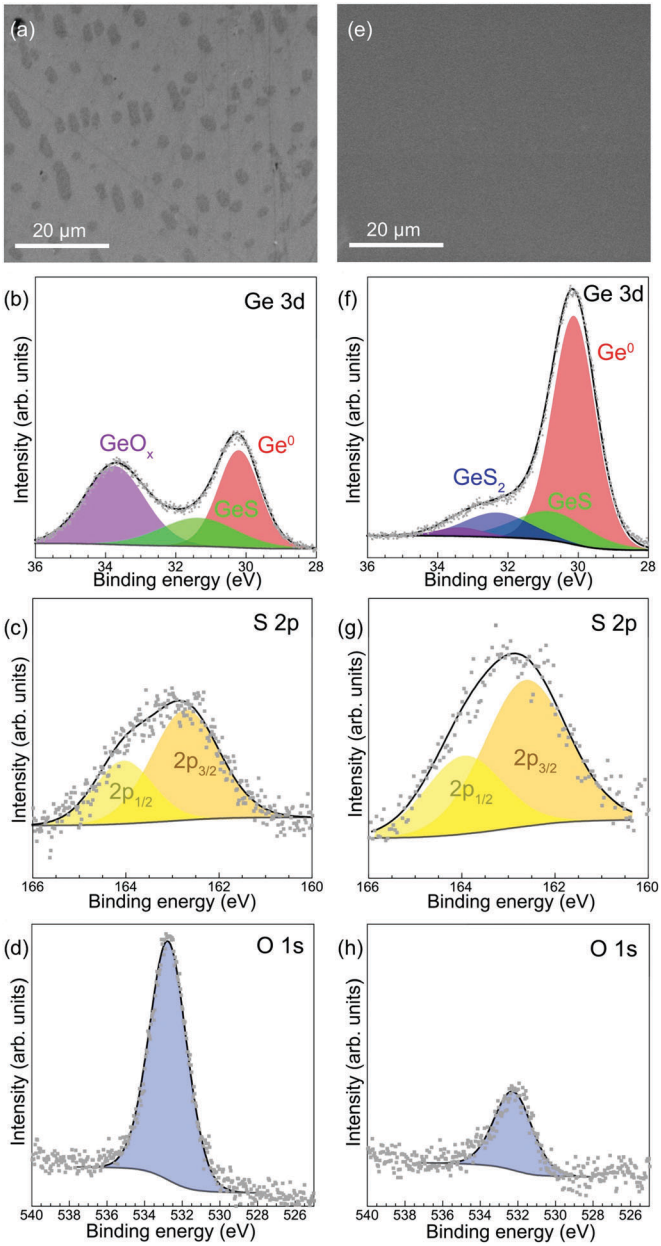

Fig. 4 SEM and XPS of the initial and later stages of germanium sulfide films produced *via* reaction of Ge(100) with sulfur vapor at 360 °C. SEM images of the surface of germanium sulfide films formed at lower sulfur vapor pressure (S crucible temperature: 120 °C) at (a) the initial and (e) later stages. (c and d) Ge 3d, S 2p and O 1s core-level spectra measured on the sample shown in (a). (f–h) Ge 3d, S 2p and O 1s core-level spectra measured on the sample shown in (e), respectively.

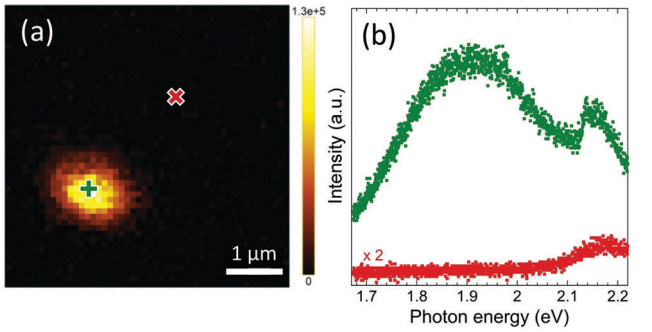

Fig. 5 Photoluminescence spectroscopy of a typical GeS flake on Ge (100). (a) PL intensity map of a typical GeS flake (see Fig. 4 (a)) excited by 532 nm light. The map shows intensity in the band between 1.8 eV and 2 eV photon energy. (b) Characteristic PL spectra obtained on the flake (green) and away from it (red).

(278 cm^{-1})[37,38] of GeS. This finding is consistent with the presence of both GeS and GeS_2 phases in samples exposed to sulfur at lower temperatures (below 400 °C). The shifts and broadening of the peaks compared with reported Raman spectra of crystalline GeS and GeS_2[37] may indicate that the reaction layers are amorphous, at least at low temperatures.[37,39]

Fig. 4 shows SEM images of the surface of the germanium sulfide films at early and later stages of their formation. In the early stages the surface has a non-uniform contrast and appears covered with nuclei or flakes of different sizes (Fig. 4(a)). XPS analysis indicates the presence of GeS and GeS_2 as well as some GeO_x, which probably results from the oxidation of the non-reacted Ge areas upon exposure to air. Photoluminescence (PL) image and spectra (Fig. 5) measured on the surface at the early stages of sulfurization show intense PL luminescence from the flakes but very low intensity in the surrounding areas. An emission peak at ~1.9 eV, close to peaks observed previously in unpolarized room temperature absorption spectra on bulk GeS, dominates the PL from the flake.[40] Away from the flake there is only weak emission at ~2.2 eV which may be attributed to oxidized Ge.[41,42] As the sulfurization progresses further, the entire surface develops uniform contrast and the germanium sulfide layer appears homogeneous (Fig. 4(e)).

A comparison between Ge(100) and Ge(111) shows no significant influence of the Ge substrate orientation on the sulfurization at moderate temperatures. In XPS spectra for Ge(100) and Ge(111) exposed to sulfur under identical conditions at 360 °C, the thicknesses of the reacted layers vary only marginally. Ge 2p spectra shown in Fig. S3 (ESI†) suggest that the reaction may be slightly further advanced for Ge(100) as compared with Ge(111) exposed to *S* under identical conditions, in agreement with the generally accepted higher reactivity of more open surfaces (*e.g.*, in adsorption or catalysis).[43] But the detected differences are small and likely within the overall experimental error.

The XPS data for Ge(100) with partial and full coverage of GeS (Fig. 4) suggest that the sulfide layer can passivate the surface and protect it against oxidation in air. For partial coverage, a sizable peak corresponding to GeO_x is found, but this peak is nearly completely suppressed in samples with full GeS coverage. This can be explained by facile oxidation of the exposed Ge surface, and passivation against oxidation by the growing Ge–sulfide film. To further probe the stability of the surface passivation under ambient conditions, we measured XPS spectra on samples exposed to air for more than 60 days. An example for GeS_x/Ge(111) formed by reaction with sulfur at 460 °C is shown in Fig. 6. Following long-term air exposure, the sample shows similar XPS characteristics as in its as-grown

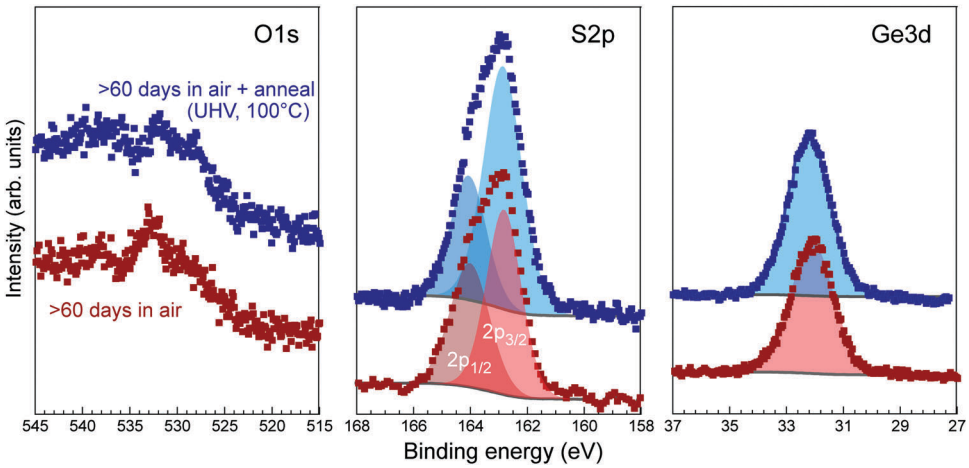

Fig. 6 XPS spectra of GeS_x/Ge(100) formed by reaction with sulfur at 460 °C, after exposure to air for >60 days, and measured under identical conditions after a brief anneal to 100 °C in vacuum. Note the intensity reduction of the O 1s peak at 532.8 eV (due to adsorbed H_2O),[44] and the concomitant increase in S 2p and Ge 3d intensity after annealing, suggesting only weakly adsorbed oxygen species.

state (*i.e.*, immediately following the reaction with sulfur). The S 2p spectrum can be fitted by two components associated with S $2p_{1/2}$ and S $2p_{3/2}$, respectively, and the Ge 3d spectrum shows only a single component due to Ge in (+4) oxidation state (GeS_2). In addition, there is a small but clearly detectable O 1s peak. Its binding energy (532.8 eV) is consistent with previous reports for H_2O,[44] suggesting adsorbed water vapor as the origin of this peak. This assignment is indeed confirmed by XPS spectra obtained under the same conditions after mild (100 °C, 15 min) annealing of the sample in the XPS chamber. After annealing, both S 2p and Ge 3d peak intensities show a slight increase, whereas the O 1s peak intensity has been reduced. The absence of other Ge 3d spectral components and of strongly bound oxygen suggests that the Ge–sulfide termination is long-term stable in air and provides a protective layer for Ge surfaces.

Conclusions

In summary, we have investigated reactions of the surface of single crystalline Ge with S vapor near ambient pressures. Exposure to S leads to the formation of Ge sulfide surface layers, whose composition and thickness at the same sulfur dose vary systematically with sample temperature. The overall behavior at low reaction temperatures can be represented by that of a three-layer system, comprising the Ge substrate, a GeS interlayer, and near-surface GeS_2. The existence of a Ge^{2+} intermediate phase suggests that the reaction limiting step is S-diffusion through the near-surface Ge–sulfides. Above 400 °C, the GeS phase is no longer detectable and exposure to sulfur gives rise to GeS_2 layers whose thickness increases with temperature. An Arrhenius analysis of the *T*-dependent GeS_2 thickness representing the rate constant of the reaction-limiting step yields an activation energy of (0.63 ± 0.08) eV, close to that for Ge oxidation by exposure to O radicals, suggesting that the reactions with oxygen and sulfur may be understood within a common framework. Finally, XPS measurements after extended ambient exposure show the ultrathin near-surface GeS_2 to be stable, and to protect the underlying Ge against oxidation in air, indicating that Ge–sulfides may provide an effective surface passivation for Ge.

Funding

This study was funded by the US National Science Foundation (Grant number DMR-1607795) and by the National Science Foundation of China (Grant numbers 61390501, 51210003, 51325204).

Conflicts of interest

The authors declare that they have no conflict of interest.

Acknowledgements

The authors acknowledge support of this work from the National Science Foundation, Division of Materials Research, under Grant No. DMR-1607795. HC, SXD and HJG acknowledge support from the National Science Foundation of China (61390501, 51210003, 51325204). We thank A. Fedorenko for assistance with the Ge–S reaction experiments.

References

1 K. F. Schuegraf and C. Hu, Reliability of thin SiO_2, *Semicond. Sci. Technol.*, 1994, **9**(5), 989.
2 C. R. Helms and E. H. Poindexter, The silicon–silicon dioxide system: its microstructure and imperfections, *Rep. Prog. Phys.*, 1994, **57**(8), 791.
3 P. W. Loscutoff and S. F. Bent, Reactivity of the germanium surface: chemical passivation and functionalization, *Annu. Rev. Phys. Chem.*, 2006, **57**, 467–495.
4 A. Prior, The field-dependence of carrier mobility in silicon and germanium, *J. Phys. Chem. Solids*, 1960, **12**(2), 175–180.

5 T. Weser, A. Bogen, B. Konrad, R. D. Schnell, C. A. Schug, W. Moritz and W. Steinmann, Chemisorption of sulfur on Ge(100), *Surf. Sci.*, 1988, **201**(1), 245–256.
6 T. Weser, A. Bogen, B. Konrad, R. D. Schnell, C. A. Schug and W. Steinmann, Photoemission surface core-level study of sulfur adsorption on Ge(100), *Phys. Rev. B: Condens. Matter Mater. Phys.*, 1987, **35**(15), 8184–8188.
7 L. M. Nelen, K. Fuller and C. M. Greenlief, Adsorption and decomposition of H_2S on the Ge(100) surface, *Appl. Surf. Sci.*, 1999, **150**(1–4), 65–72.
8 G. Anderson, M. Hanf, P. Norton, Z. Lu and M. Graham, The S-passivation of Ge(100)-(1 × 1), *Appl. Phys. Lett.*, 1995, **66**(9), 1123–1125.
9 P. Lyman, O. Sakata, D. Marasco, T.-L. Lee, K. Breneman, D. Keane and M. Bedzyk, Structure of a passivated Ge surface prepared from aqueous solution, *Surf. Sci.*, 2000, **462**(1), L594–L598.
10 T. Hanrath and B. A. Korgel, Chemical surface passivation of Ge nanowires, *J. Am. Chem. Soc.*, 2004, **126**(47), 15466–15472.
11 D. Bodlaki, H. Yamamoto, D. Waldeck and E. Borguet, Ambient stability of chemically passivated germanium interfaces, *Surf. Sci.*, 2003, **543**(1), 63–74.
12 R. Gatensby, N. McEvoy, K. Lee, T. Hallam, N. C. Berner, E. Rezvani, S. Winters, M. O'Brien and G. S. Duesberg, Controlled synthesis of transition metal dichalcogenide thin films for electronic applications, *Appl. Surf. Sci.*, 2014, **297**, 139–146.
13 D. S. Kong, H. T. Wang, J. J. Cha, M. Pasta, K. J. Koski, J. Yao and Y. Cui, Synthesis of MoS_2 and $MoSe_2$ Films with Vertically Aligned Layers, *Nano Lett.*, 2013, **13**(3), 1341–1347.
14 M. R. Laskar, L. Ma, S. Kannappan, P. S. Park, S. Krishnamoorthy, D. N. Nath, W. Lu, Y. Y. Wu and S. Rajan, Large area single crystal (0001) oriented MoS_2, *Appl. Phys. Lett.*, 2013, **102**, 25.
15 Y. J. Zhan, Z. Liu, S. Najmaei, P. M. Ajayan and J. Lou, Large-Area Vapor-Phase Growth and Characterization of MoS_2 Atomic Layers on a SiO_2 Substrate, *Small*, 2012, **8**(7), 966–971.
16 C. R. Wu, X. R. Chang, T. W. Chu, H. A. Chen, C. H. Wu and S. Y. Lin, Establishment of 2D Crystal Heterostructures by Sulfurization of Sequential Transition Metal Depositions: Preparation, Characterization, and Selective Growth, *Nano Lett.*, 2016, **16**(11), 7093–7097.
17 B. Meyer, Elemental sulfur, *Chem. Rev.*, 1976, **76**(3), 367–388.
18 G. Beamson and D. Briggs, High Resolution X. P. S. of Organic Polymers: The Scienta ESCA300 Database, *J. Chem. Educ.*, 1993, **70**(1), A25.
19 P. Ponath, A. B. Posadas and A. A. Demkov, Ge(001) surface cleaning methods for device integration, *Appl. Phys. Rev.*, 2017, **4**(2), 021308.
20 S. R. Amy, Y. J. Chabal, F. Amy, A. Kahn, C. Krugg and P. Kirsch, Wet chemical cleaning of germanium surfaces for growth of high-*k* dielectrics, *Mater. Res. Soc. Symp. Proc.*, 2006, **917**, 0917 E01.
21 B. Onsia, T. Conard, S. De Gendt, M. Heyns, I. Hoflijk, P. Mertens, M. Meuris, G. Raskin, S. Sioncke and I. Teerlinck, A study of the influence of typical wet chemical treatments on the germanium wafer surface, *Solid State Phenom.*, 2005, **103**, 27–30.
22 K. Prabhakaran and T. Ogino, Oxidation of Ge(100) and Ge(111) surfaces: an UPS and XPS study, *Surf. Sci.*, 1995, **325**(3), 263–271.
23 N. Tabet, M. Faiz, N. M. Hamdan and Z. Hussain, High resolution XPS study of oxide layers grown on Ge substrates, *Surf. Sci.*, 2003, **523**(1–2), 68–72.
24 N. A. Tabet, M. A. Salim and A. L. Al-Oteibi, XPS study of the growth kinetics of thin films obtained by thermal oxidation of germanium substrates, *J. Electron Spectrosc.*, 1999, **101–103**, 233–238.
25 F. d'Heurle and P. Gas, Kinetics of formation of silicides: A review, *J. Mater. Res.*, 1986, **1**(01), 205–221.
26 M. Tinani, A. Mueller, Y. Gao, E. Irene, Y. Hu and S. Tay, In situ real-time studies of nickel silicide phase formation, *J. Vac. Sci. Technol., B: Microelectron. Nanometer Struct.–Process., Meas., Phenom.*, 2001, **19**(2), 376–383.
27 K. Ogata, E. Sutter, X. Zhu and S. Hofmann, Ni–silicide growth kinetics in Si and Si/SiO_2 core/shell nanowires, *Nanotechnology*, 2011, **22**(36), 365305.
28 M. Dreiling, Quantitative surface measurements of metal oxide powders by X-ray photoelectron spectroscopy (XPS), *Surf. Sci.*, 1978, **71**(2), 231–246.
29 C. J. Powell and D. R. Penn, Calculations of Electron Inelastic Mean Free Paths, *Surf. Interface Anal.*, 1991, **17**, 926.
30 A. Jain, S. P. Ong, G. Hautier, W. Chen, W. D. Richards, S. Dacek, S. Cholia, D. Gunter, D. Skinner, G. Ceder and K. A. Persson, Commentary: The Materials Project: A materials genome approach to accelerating materials innovation, *APL Mater.*, 2013, **1**(1), 011002.
31 J. Málek, The thermal stability of chalcogenide glasses, *J. Therm. Anal. Calorim.*, 1993, **40**(1), 159–170.
32 B. E. Deal and A. Grove, General relationship for the thermal oxidation of silicon, *J. Appl. Phys.*, 1965, **36**(12), 3770–3778.
33 M. Kobayashi, G. Thareja, M. Ishibashi, Y. Sun, P. Griffin, J. McVittie, P. Pianetta, K. Saraswat and Y. Nishi, Radical oxidation of germanium for interface gate dielectric GeO_2 formation in metal–insulator–semiconductor gate stack, *J. Appl. Phys.*, 2009, **106**(10), 104117.
34 X. Wang, Z. Zhao, J. Xiang, W. Wang, J. Zhang, C. Zhao and T. Ye, Experimental investigation on oxidation kinetics of germanium by ozone, *Appl. Surf. Sci.*, 2016, **390**, 472–480.
35 C. Wagner, L. Davis, M. Zeller, J. Taylor, R. Raymond and L. Gale, Empirical atomic sensitivity factors for quantitative analysis by electron spectroscopy for chemical analysis, *Surf. Interface Anal.*, 1981, **3**(5), 211–225.
36 J. P. Berube, S. H. Messaddeq, M. Bernier, I. Skripachev, Y. Messaddeq and R. Vallee, Tailoring the refractive index of Ge–S based glass for 3D embedded waveguides operating in the mid-IR region, *Opt. Express*, 2014, **22**(21), 26103–26116.
37 S. M. Tan, C. K. Chua, D. Sedmidubsky, Z. C. Sofer and M. Pumera, Electrochemistry of layered GaSe and GeS: applications to ORR, OER and HER, *Phys. Chem. Chem. Phys.*, 2016, **18**(3), 1699–1711.
38 C. Li, L. Huang, G. P. Snigdha, Y. Yu and L. Cao, Role of boundary layer diffusion in vapor deposition growth of chalcogenide nanosheets: the case of GeS, *ACS Nano*, 2012, **6**(10), 8868–8877.

39 C. C. Huang, D. Hewak and J. Badding, Deposition and characterization of germanium sulphide glass planar waveguides, *Opt. Express*, 2004, **12**(11), 2501–2506.
40 D. Bletskan, I. Madyar, S. Mikulaninets and M. Y. Sichka, Electrical and photoelectric properties of GeS layered crystals grown by different techniques, *Inorg. Mater. (Transl. of Neorg. Mater.)*, 2000, **36**(6), 544–550.
41 Y. Kanemitsu, Mechanism of visible photoluminescence from oxidized silicon and germanium nanocrystallites, *Thin Solid Films*, 1996, **276**(1–2), 44–46.
42 M. Peng, Y. Li, J. Gao, D. Zhang, Z. Jiang and X. Sun, Electronic structure and photoluminescence origin of single-crystalline germanium oxide nanowires with green light emission, *J. Phys. Chem. C*, 2011, **115**(23), 11420–11426.
43 S. L. Horswell, A. L. N. Pinheiro, E. R. Savinova, M. Danckwerts, B. Pettinger, M.-S. Zei and G. Ertl, A Comparative Study of Hydroxide Adsorption on the (111), (110), and (100) Faces of Silver with Cyclic Voltammetry, *Ex Situ* Electron Diffraction, and *In Situ* Second Harmonic Generation, *Langmuir*, 2004, **20**(25), 10970–10981.
44 N. Martensson, P. A. Malmquist, S. Svensson, E. Basilier, J. J. Pireaux, U. Gelius and K. Siegbahn, Molecular and Solid Water, a Comparative ESCA Study, *Nouv. J. Chim.*, 1977, **1**(3), 191–195.

